

## Article

# Friction Properties of the Heat-Treated Electroless Ni Coatings Embedded with c-BN Nanoparticles

Mara Kandeва<sup>1,2</sup>, Mihail Zagorski<sup>1</sup> , Ružica Nikolić<sup>3</sup> , Blaža Stojanović<sup>4</sup> , Adrian But<sup>5</sup>, František Botko<sup>6</sup> , Ján Piteľ<sup>6</sup>  and Aleksandar Vencl<sup>7,2,\*</sup> 

<sup>1</sup> Faculty of Industrial Technology, Technical University of Sofia, 8 Kliment Ohridski Blvd, 1000 Sofia, Bulgaria; kandevam@gmail.com (M.K.); mihail.zagorski.tu@gmail.com (M.Z.)

<sup>2</sup> South Ural State University, Lenin prospekt 76, 454080 Chelyabinsk, Russia

<sup>3</sup> Research Center, University of Žilina, Univerzitna 8215/1, 010 26 Žilina, Slovakia; ruzica.nikolic@uniza.sk

<sup>4</sup> University of Kragujevac, Faculty of Engineering, Sestre Janjić 6, 34000 Kragujevac, Serbia; blaza@kg.ac.rs

<sup>5</sup> Faculty of Mechanical Engineering, Politehnica University of Timișoara, Bulevardul Mihai Viteazu 1, 300222 Timișoara, Romania; adi.but@gmail.com

<sup>6</sup> Faculty of Manufacturing Technologies, Technical University of Košice, Bayerova 1, 080 01 Prešov, Slovakia; frantisek.botko@tuke.sk (F.B.); jan.pitel@tuke.sk (J.P.)

<sup>7</sup> University of Belgrade, Faculty of Mechanical Engineering, Kraljice Marije 16, 11120 Belgrade, Serbia

\* Correspondence: avenc1@mas.bg.ac.rs

**Abstract:** The nickel (Ni) coatings without and with embedded (5–7 vol. %) cubic boron nitride (c-BN) nanoparticles (10 nm in diameter) were deposited on carbon steel substrate by an electroless plating process. Coatings were tested in as-deposited and heat-treated (heating at 300 °C for 6 h) conditions. Coating structure characterisation was performed, as well as hardness and roughness measurements. Friction properties were tested in dry and in water (seawater) lubricated contact conditions, with bronze as a counter-body material. Both static and kinetic coefficients of friction were measured for two different surface texture preparations (initial and working). The first surface texture simulated the running-in condition, and the second surface texture represented the steady-state conditions. The enhancement of the abrasive and erosive wear resistance of heat-treated electroless Ni coatings with embedded c-BN nanoparticles was already proved in our previous studies. This study aims to investigate those influences on friction properties of electroless Ni coatings in different sliding conditions. The results show that the coefficients of friction did not differ too much between the coatings and that the surface roughness and presence of seawater had a much stronger influence.

**Keywords:** electroless nickel coatings; cubic boron nitride; nanoparticles; seawater; friction



**Citation:** Kandeва, M.; Zagorski, M.; Nikolić, R.; Stojanović, B.; But, A.; Botko, F.; Piteľ, J.; Vencl, A. Friction Properties of the Heat-Treated Electroless Ni Coatings Embedded with c-BN Nanoparticles. *Coatings* **2022**, *12*, 1008.

<https://doi.org/10.3390/coatings12071008>

Academic Editors: Zhao Zhang and Emerson Coy

Received: 20 May 2022

Accepted: 13 July 2022

Published: 18 July 2022

**Publisher's Note:** MDPI stays neutral with regard to jurisdictional claims in published maps and institutional affiliations.



**Copyright:** © 2022 by the authors. Licensee MDPI, Basel, Switzerland. This article is an open access article distributed under the terms and conditions of the Creative Commons Attribution (CC BY) license (<https://creativecommons.org/licenses/by/4.0/>).

## 1. Introduction

Electroless nickel (Ni) plating is the deposition process in which mainly chemical energy is applied, and the typical thickness of the obtained coating varies from 2 to 125 μm [1]. The process was patented more than 70 years ago [2] and since then it found application in many industries, mainly where enhanced wear and/or corrosion resistance or improved magnetic properties are needed [3,4]. Depending on the phosphorus content, electroless Ni coatings can be classified as low-phosphorus (1–3 wt. % P), low-medium-phosphorus (3–6 wt. % P), medium-phosphorus (6–9 wt. % P) and high-phosphorus (9–13 wt. % P) alloys [5]. Phosphorus content, together with the heat treatment parameters, has a strong influence on coating performance. The heat treatment alters the hardness, structure and morphology of a coating [6,7], thereby affecting its wear and corrosion resistance.

The increase in the hardness and wear resistance of these coatings is mainly due to the transformation of nickel from the amorphous to crystalline structure and the production of the hard Ni<sub>3</sub>P phase [7,8]. Furthermore, electroless Ni coatings can be deposited with incorporated micro- and nano-sized particles and fibres such as SiO<sub>2</sub>, Al<sub>2</sub>O<sub>3</sub>, SiC, B<sub>4</sub>C,

diamond, WC, Si<sub>3</sub>N<sub>4</sub>, ZnO, ZrO<sub>2</sub>, TiO<sub>2</sub>, etc. [6], producing a composite coating. The influences of nano-sized particle incorporation, their type as well as matrix types on the mechanical properties of composites have been widely investigated [9,10].

Boron nitride particles are rarely incorporated in Ni-based composites, and one of the reasons could be the relatively high difference in thermal expansion coefficients of the Ni matrix and BN particles. The BN particles are mainly used in the form of hexagonal boron nitride (h-BN) [11,12]. This form is relatively soft and like graphite is used as a solid lubricant additive. On the other hand, cubic boron nitride (c-BN) is much harder and comparable to diamond, with an excellent combination of mechanical properties [13,14].

Interestingly, there are significantly fewer studies focused on c-BN as a reinforcing phase in the composite coatings. In our previous studies, we proved enhanced abrasive and erosive wear resistance of the heat-treated electroless Ni coatings embedded with c-BN nanoparticles [1,15], but there is a lack of information on the frictional performance of those coatings. Therefore, the aim of the presented study was to investigate the influence of the heat treatment and addition of c-BN nanoparticles on the static and kinetic coefficients of friction in dry and water (seawater) lubricated contact conditions in both working regimes, i.e., in running-in and in steady-state conditions.

## 2. Experimental Details

### 2.1. Materials

All coatings were produced by the electroless plating process. Composite coatings had incorporated 5–7 vol. % c-BN commercially obtained nanoparticles (10 nm in diameter). This volume percentage was chosen to be the same as in our previous investigations when we proved enhanced abrasive and erosive wear resistance of the coatings [1,15]. Nanoparticles were purchased from American Elements (Los Angeles, CA, USA), having 99% purity, solid appearance, spherical shape and cubic morphology. Due to their small size, most of the particles were grouped in agglomerations. The substrate material for all the coatings was a carbon steel CТ3КП (GOST 380), in disk shape of 100 mm diameter and 2.5 mm thickness, with following chemical composition: Fe-0.4C-0.2Si-0.55Mn-0.3Cr-0.3Ni-0.45P-0.045S (wt. %). SEM images of the used c-BN nanoparticles and steel substrate were not shown since they are commercially available materials with controlled properties. The microhardness of the substrate was 135 HV 0.05, and surface roughness was  $Ra = 0.089 \mu\text{m}$ .

Heat treatment (heating at 300 °C for 6 h) was applied to half of the samples to improve their structural and mechanical properties. Therefore, a total of four samples of two different electroless Ni coatings (with and without embedded c-BN nanoparticles) were examined. Designations and descriptions of the tested samples are shown in Table 1. The literature data show that the optimum temperature range for one-hour heat treatment is 345 to 400 °C. However, increased mechanical properties can be also obtained at lower temperatures but longer times are required [16]. Although the heat treatment significantly improves the wear resistance of the coating, if higher temperatures have been used an increase in the porosity of the coating generally would occur with a corresponding decrease in corrosion resistance [16,17].

**Table 1.** Designation and thickness of the tested samples.

No.	Designation	Description	Thickness, $\mu\text{m}$
1	Ni	As-deposited coating without nanoparticles	26.2
2	Ni <sup>HT</sup>	Heat-treated coating without nanoparticles	12.8
3	Ni-BN	As-deposited coating with c-BN nanoparticles	22.8
4	Ni-BN <sup>HT</sup>	Heat-treated coating with c-BN nanoparticles	9.5

The thickness of the coatings was measured in 5 points by Pocket-LEPTOSKOP 2021 Fe, and the calculated average thickness values are also shown in Table 1. As can be noticed, thicknesses of the as-deposited samples of approx. 24.5  $\mu\text{m}$  were about two times higher

than the thickness of the heat-treated samples (approx. 11.1  $\mu\text{m}$ ). Further, the incorporation of c-BN nanoparticles also induced slightly lower thicknesses.

## 2.2. Methods of Characterization

The microstructure analysis of the as-deposited and heat-treated electroless Ni coating with embedded c-BN nanoparticles was performed by scanning electron microscopy (SEM) and their composition was checked with the energy dispersive X-ray spectroscopy (EDS). The microhardness (HV 0.5) measurements were performed using a Vickers microhardness tester under a load of 500 g and a dwell time of 15 s. At least three measurements were made for each sample and average values are presented.

The roughness was examined with mechanical profilometer TESA Rugosurf 10G in two perpendicular directions and the mean value was calculated. Each of the four coatings from Table 1 was tested with two surface roughness conditions (initial and working), simulating the running-in and steady-state working regime. Initial roughness was as-deposited roughness, i.e., it was measured after the deposition of the coating. Working roughness was measured after the purposely smoothing of the surfaces on Taber Abraser with abrading wheel Calibrase<sup>®</sup> CS-10 [18] and fixed load (2.45 N), sliding speed (approx. 0.24 m/s) and abrading time (1000 s) for all samples.

The coefficient of friction testing was performed on the laboratory device, which is described elsewhere [18]. Three different normal loads were used (10, 15 and 20 N) in both, dry contact conditions and seawater-lubricated contact conditions. The counter-body was the same in all tests: bronze (264.4 HV 0.05;  $R_a = 0.31 \mu\text{m}$ ) cylinder of 10 mm diameter and 20 mm height, i.e., geometrical contact area was approximately 78.5 mm<sup>2</sup>. For each test condition, five replicate tests were performed and average values are presented. Water used for lubrication was natural seawater taken from the Black Sea, which has a relatively low salinity of 1.79% compared to the average salinity in the world's oceans (approx. 3.5%). Concentrations of major dissolved ions (with the concentration of 100 mg per 1 l or more) in used seawater are shown in Table 2.

**Table 2.** Concentrations of major dissolved ions in used seawater.

Component	Concentration, g/L
Cl <sup>-</sup>	9.89
Na <sup>+</sup>	5.44
SO <sub>4</sub> <sup>2-</sup>	1.38
Mg <sup>2+</sup>	0.48
Ca <sup>2+</sup>	0.27
K <sup>+</sup>	0.21
HCO <sub>3</sub> <sup>-</sup>	0.16

## 3. Results and Discussion

### 3.1. Microstructure and Composition

The typical structure of the as-deposited electroless Ni coatings is nodular with surface morphology in the cauliflower-like shape [6,19]. As-deposited coatings with the low phosphorus content show a nanocrystalline structure, while the high phosphorus content coatings are amorphous or microcrystalline [6,8]. The amorphous structure occurs due to an excess of phosphorus at grain boundaries of Ni, which prevents its nucleation [7]. Heat treatment of electroless Ni coatings results in a transformation of the amorphous to a crystalline structure. Recrystallization of microcrystalline nickel occurs [7] and as-deposited nodules increase in size, giving the rise to a coarse-grained structure. In addition, phosphides and borides are precipitated [6].

The surface morphology of as-deposited electroless Ni coating with embedded c-BN nanoparticles, at different magnifications, is shown in Figure 1. The addition of the nano-sized c-BN particles prevented formation of a coarse microcrystalline structure typical for high phosphorus content coating; instead, the coatings had a more desirable finer

structure. This means that the nanoparticles acted as the structure modifiers. The chemical composition of as-deposited electroless Ni coating with embedded c-BN nanoparticles is performed with EDS analysis (Figure 2). The presence of chemical elements Ni, P, B and N confirms that the c-BN nanoparticles were successfully incorporated into the Ni coating.

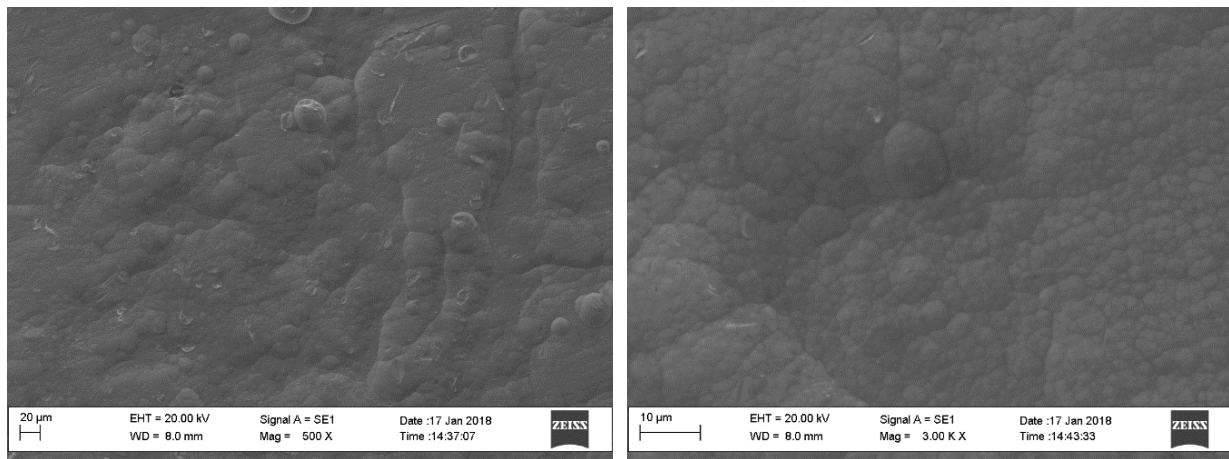


**Figure 1.** Surface morphology (SEM images) of as-deposited electroless Ni coating with embedded c-BN nanoparticles (Ni-BN) at different magnifications.

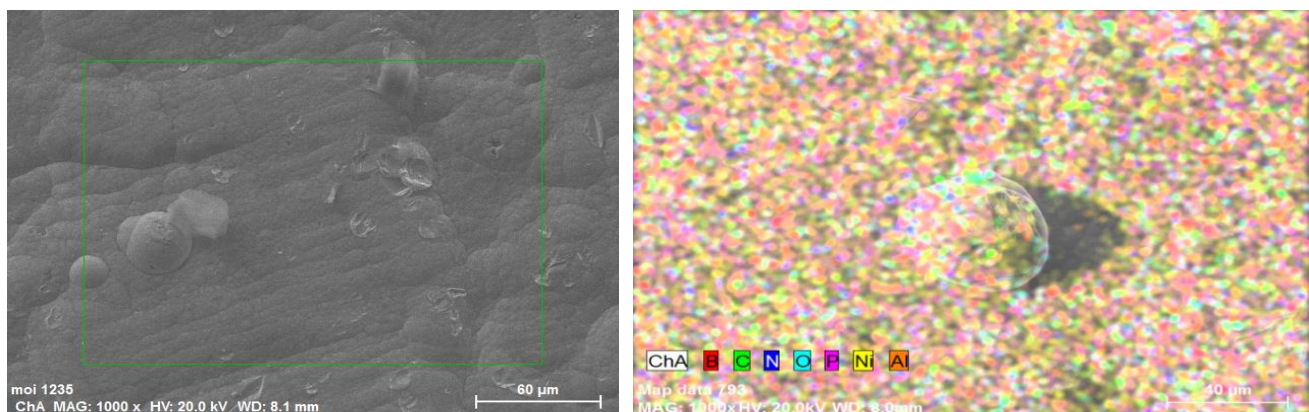


**Figure 2.** EDS analysis of the marked area on surface of as-deposited electroless Ni coating with embedded c-BN nanoparticles (Ni-BN).

The heat treatment of electroless Ni coatings with embedded c-BN particles resulted in transformation to crystalline structure and precipitation of the hard  $\text{Ni}_3\text{P}$  and  $\text{Ni}_3\text{B}$  phases [8,20]. The comparison of the surface morphology of the as-deposited and heat-treated electroless Ni coating with embedded c-BN nanoparticles was performed on SEM images of the same magnification; the heat-treated coatings should have the finer crystal structure (Figure 3) compared to that of the as-deposited coatings (Figure 1). The recrystallization process that took place during the heat treatment was probably related to the higher rate of formation of crystal nuclei, compared to the rate of their growth, due to which more nodules were formed.

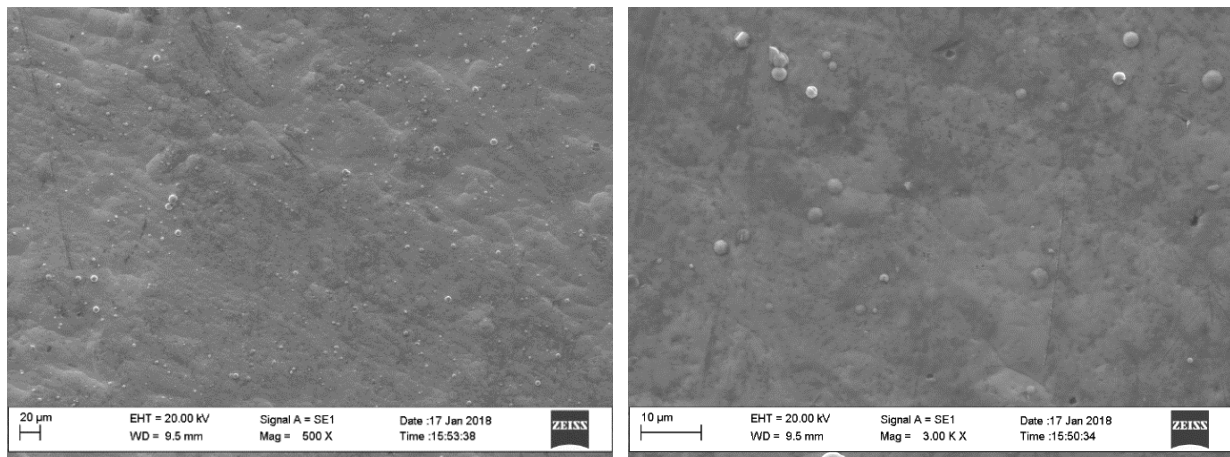


**Figure 3.** Surface morphology (SEM images) of the heat-treated electroless Ni coating with embedded c-BN nanoparticles (Ni-BN<sup>HT</sup>) at different magnifications.

The chemical composition of the heat-treated electroless Ni coating with embedded c-BN nanoparticles is also performed by EDS analysis (Figure 4) on the SEM image of the same magnification as the as-cast coatings. The analysis showed the presence of the same chemical elements Ni, P, B and N and also the presence of Fe. The presence of Fe is probably due to the diffusion from the substrate (carbon steel). The EDS mapping of the composition of the rectangular area marked on Figure 4 is performed and the results are given in Figure 5. Single nodules of the formed morphology after the heat treatments were also analysed by the EDS (Figure 6). It was confirmed that it represents Ni coating with a high phosphorus content (above 10 wt. %).

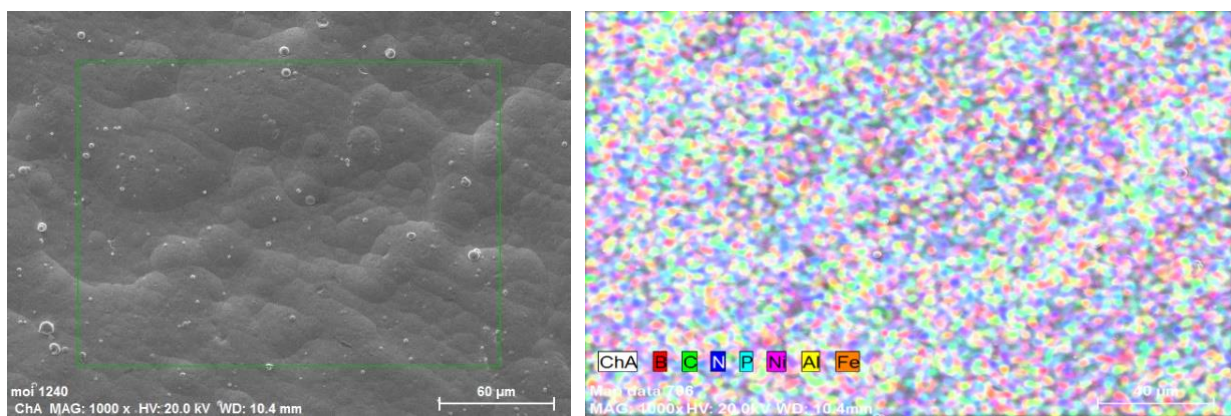


**Figure 4.** EDS analysis of the marked area on surface of the heat-treated electroless Ni coating with embedded c-BN nanoparticles (Ni-BN<sup>HT</sup>).

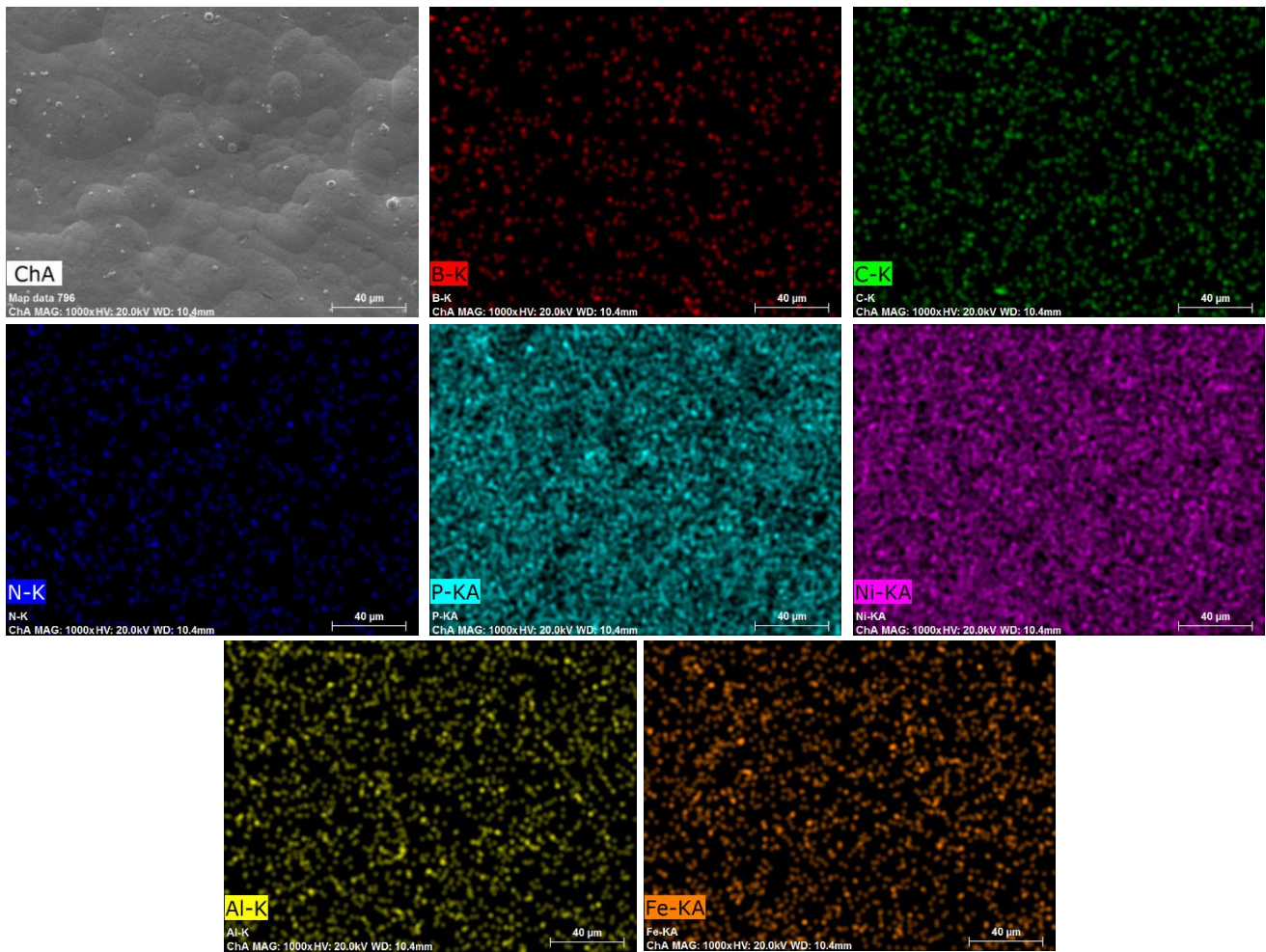


Figure 5. EDS mapping of composition of the rectangular area marked in Figure 4.

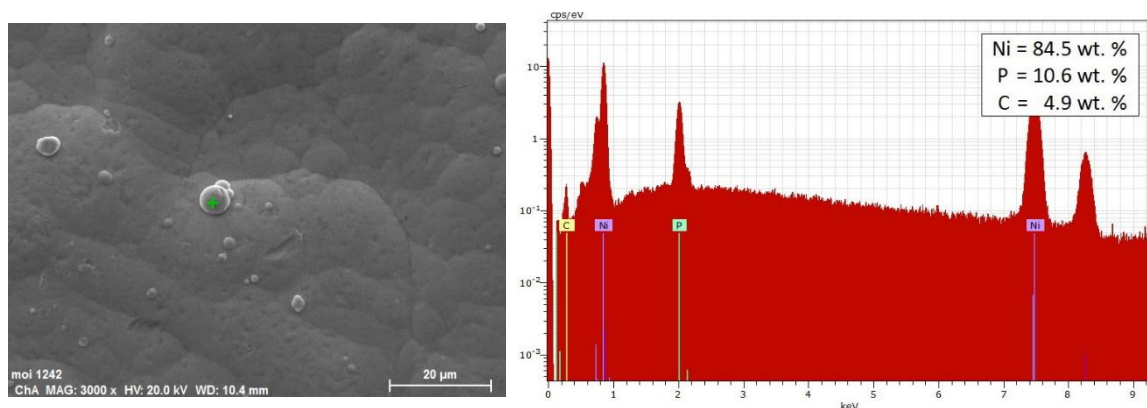


Figure 6. EDS analysis of the single nodule at the surface of the heat-treated electroless Ni coating with embedded c-BH nanoparticles (Ni-BN<sup>HT</sup>).

### 3.2. Microhardness and Surface Roughness

Results of the microhardness measurements are shown in Table 3 and represent the average values. The obtained values are in accordance with the phosphorus content and with literature data [8]. Typical Knoop microhardness values of as-deposited electroless Ni coatings range from 500 to 720 HK 0.1, where the lower values refer to higher phosphorus content [16]. Heat treatment increased hardness values of both Ni coatings (without and with embedded c-BN nanoparticles). The increment in hardness of Ni coating without

nanoparticles is attributed to the crystallization of nickel and precipitation of the hard  $\text{Ni}_3\text{P}$  phase [7]. The hardness of Ni coating with embedded nanoparticles was additionally increased upon the heat treatment due to the precipitation of the hard  $\text{Ni}_3\text{B}$  phase, as well [20]. The average increase in microhardness due to heat treatment was relatively low, i.e., 47 HV 0.5 (9%), but it is known that the long period of heat treatment, and in our case it was 6 h, could induce the decrease in hardness due to the nickel grain growth and the phosphides coarsening [6,8].

**Table 3.** Microhardness and surface roughness of the tested samples.

No.	Designation	Microhardness HV 0.5	Surface Roughness ( $R_a$ ), $\mu\text{m}$	
			Initial (as-Deposited)	Working (after Smoothing)
1	Ni	538		
2	$\text{Ni}^{\text{HT}}$	560		
3	Ni-BN	518	0.413	0.221
4	$\text{Ni-BN}^{\text{HT}}$	590		

The surface roughness values were similar for all the samples, so only the averaged values are presented (Table 3). It can be noticed that the roughness has changed significantly after the purposeful smoothing of the asperities with an abrading wheel, i.e., the roughness is almost halved in that case. The aim was to simulate the operating conditions of plain bearings where the roughness of  $R_a < 0.4 \mu\text{m}$  is generally recommended, while even lower values of  $R_a = 0.20\text{--}0.25 \mu\text{m}$  are recommended for crankshaft sleeves in internal combustion engines [21].

### 3.3. Dry Contact Friction

The obtained values of the static and kinetic coefficients of friction (COF) of coatings with initial roughness, tested at different normal loads in dry contact conditions, are presented in Figure 7. The repeatability of the results, in terms of averaged standard deviation, was good, i.e., below 5%. There is no noticeable effect of the normal load on COF values, which is in accordance with classical laws for dry contact friction. Heat treatment and addition of c-BN nanoparticles also did not show any regularity regarding COF values, i.e., different materials (coatings) showed similar COF values. The only difference that could be noticed is between the static and kinetic COF values. The average value for the static COF was 0.271 and for kinetic COF it was 0.247, so the difference is 0.024 (about 8.8%). This difference is lower than the usual differences of 20% to 30% [19].

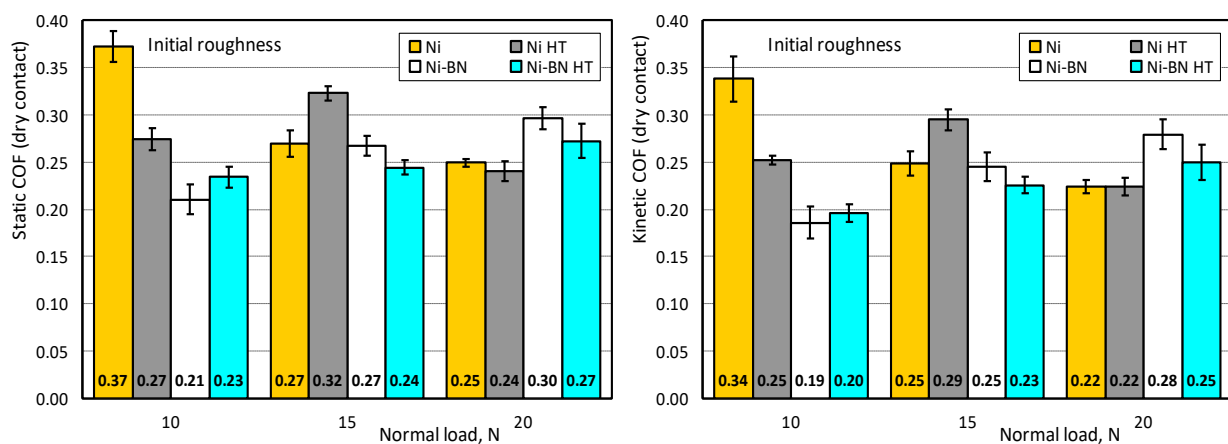


**Figure 7.** Static and kinetic coefficient of friction (COF) values and appropriate standard deviations of coatings with initial roughness, tested at different normal loads in dry contact conditions.

The obtained COF values more or less correspond to the experimental values for metal–metal contact under dry sliding conditions [22]. Similar values were also obtained in some

of our previous studies of electroless Ni coatings embedded with SiC nanoparticles [18,19]. Although the heat treatment and addition of c-BN nanoparticles affected the increase in hardness (Table 3) as well as a significant increase in abrasive wear and erosive wear resistance (heat treatment increased abrasive wear resistance by approx. 2.5 times and erosive wear resistance by approx. 2.0 times, while the addition of c-BN nanoparticles increased abrasive wear resistance by approx. 1.8 times and erosive wear resistance by approx. 1.3 times) [1], their negative impact on COF (increase in COF) was not observed. This is not in correlation with the review made by Sahoo and Das [6], who found that the addition of hard particles like B<sub>4</sub>C and SiC has a tendency to increase the COF of electroless Ni coatings. This is most probably because the counter-body (bronze) had significantly lower hardness (more than twice) than all the tested coatings. This lower hardness caused that the ploughing and shearing of the adhesive junctions occurs mainly through the bronze, so the COF is controlled by the bronze. This is why the COF values did not differ too much between different coatings. A similar regularity was obtained in the previous study [19], where the material with the lowest hardness showed the lowest COF.

The coefficient of friction testing in dry contact conditions was also performed for coatings whose surface was purposely smoothed, thus simulating the steady-state conditions. The results for these coatings are shown in Figure 8. The repeatability of the results, in terms of averaged standard deviation, was acceptable, i.e., around 8%. The results showed similar regularities regarding the influence of normal load, heat treatment and addition of c-BN nanoparticles, i.e., their influences on static or kinetic COF could not be noticed. Therefore, like for coatings with initial roughness, the average values can be accepted. For the static COF, it was 0.173, for kinetic COF it was 0.157 and the difference was 0.016, i.e., about 9.7%. This difference was also relatively small and still lower than the usual differences of 20% to 30% [19].

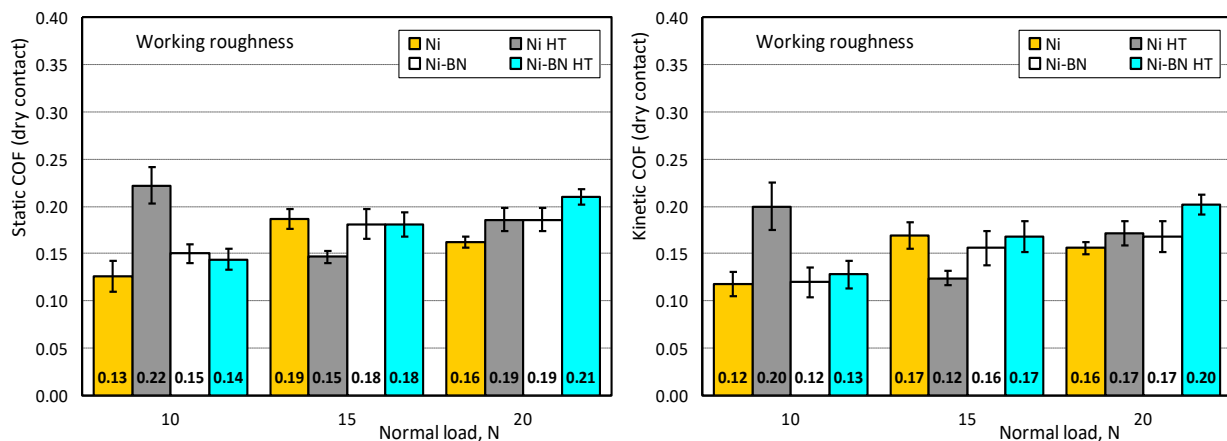


**Figure 8.** Static and kinetic coefficient of friction (COF) values and appropriate standard deviations of coatings with working roughness, tested at different normal loads in dry contact conditions.

Comparing the values of both static and kinetic COF obtained for the same coating with different surface conditions (initial and working roughness), it could be noticed that the values are much lower for the working roughness conditions (0.173 vs. 0.271 for the static COF and 0.157 vs. 0.247 for the kinetic COF). This is in line with the results obtained for various roughness of surfaces machined with different machining processes, which show that the static COF value is higher if contact surfaces have higher roughness parameters [23]. In this study, the average surface roughness of the as-deposited coatings (initial roughness) was 0.413  $\mu\text{m}$  (Table 3), which is relatively high. In addition to this, the bronze counter-body was more than two times softer than any coating; so, the dominant component of friction should be the ploughing (deformation) component. With the smoothing of the coatings (working roughness), average roughness was reduced to 0.221  $\mu\text{m}$  and most probably that the distribution of the material in the surface layer was better (higher bearing area). This

increased the real area of contact and the adhesive component of friction, but at the same time had a much higher influence on decreasing the ploughing component of friction, so in total the COF (static and kinetic) was lower.

The importance of the surface topography in controlling the friction during the sliding was confirmed by Uday Venkat Kiran et al. [7]. They measured kinetic COF on steel ball-on-plate tribometer at linearly reciprocating sliding under the normal load of 10 N for as-deposited and heat-treated electroless Ni coating. Like in this study, there was a very low influence of the heat treatment on COF, and for both coatings COF was around 0.21, i.e., very similar to the values obtained in this study (0.157 and 0.247).

### 3.4. Seawater Lubricated Contact Friction

The obtained values of the kinetic COF for coatings with initial and working roughness, tested at different normal loads in seawater-lubricated contact conditions, are presented in Figure 9. The repeatability of the results, in terms of averaged standard deviation, was acceptable, as well, i.e., below 5% (initial roughness) and around 8% (working roughness). The heat treatment and the addition of c-BN nanoparticles also did not show any noticeable influence on the kinetic COF values, so the average value of 0.235 (initial roughness) and 0.139 (working roughness) can be accepted. These values are slightly lower than the values obtained in dry contact conditions, which suggest a beneficial influence of the seawater lubrication on the COF. A similar influence of water lubrication was noticed by Niu et al. [24] for several Ti alloys in contact with the WC-Co counter-body. They used a ball-on-plate tribometer in linearly reciprocating sliding mode with a normal load of 3 N. The results showed that COF in dry sliding conditions was between 0.34 and 0.42 while in pure water-lubricated conditions the COF decreased and was between 0.26 and 0.30.

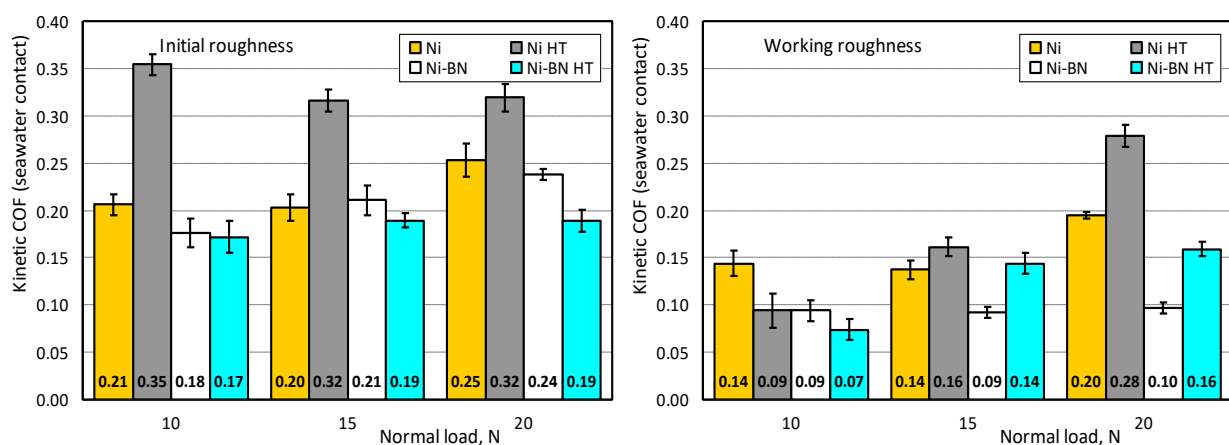


**Figure 9.** Kinetic coefficient of friction (COF) values and appropriate standard deviations of coatings with initial and working roughness, tested at different normal loads in seawater-lubricated contact conditions.

Generally, the presence of water can significantly affect the corrosion and wear of the contact surfaces [25], but relatively low values of the COF, which were obtained, indicate that there was no intensive corrosion. The example of the negative influence of corrosion on the COF is presented by Miura et al. [26], who compared the static COF of uncorroded (tests in the air) and corroded (tests in seawater and in distilled water) specimens. In the case of uncorroded surfaces, COF was 0.24–0.28 and for corroded specimens it rose to 0.46–0.55. In this study, the duration of the test was very short and there was not enough time for the corrosion to occur. In addition, the salinity of the used seawater was lower than the average salinity in the world’s oceans, and lower salinity also means lower corrosion risk [27].

The obtained values for coatings with working roughness (around 0.139) indicate the presence of a boundary lubrication regime since the literature data for the COF in

the boundary lubrication regime are between 0.05 and 0.15 [28]. Similar COF values of Cr/graphite-like carbon coatings, lubricated with the seawater and tested on a ball-on-plate tribometer in linearly reciprocating sliding mode with a normal load of 5 N, were obtained for contacts with various ceramic [29] and metal [30] counter-body materials. Opposite of the other results presented in this study, coatings with low (working) roughness lubricated with seawater showed dependence on the applied normal load (Figure 9). The average values for all the coatings tested at different loads are: 0.101 (for 10 N), 0.134 (for 15 N) and 0.182 (for 20 N). This slight increase in the COF with the increase in normal load fits the Stribeck curve in the area of boundary lubrication.

#### 4. Conclusions

The obtained results for the friction behaviour of different electroless Ni coatings showed that the heat treatment and addition of c-BN nanoparticles did not have the impact of the same scale as it had on the abrasive and erosive wear resistance of the same coatings. These properties were determined in our previous studies and were significantly improved by the heat treatment and addition of c-BN nanoparticles. Although it was expected, the increase in the COF was not noticed, i.e., all coatings showed similar values of the static and kinetic COF regardless of the testing conditions.

The main influence on friction values of the tested coatings had surface texture conditions, expressed through the surface roughness. Coatings that were smoothed during the running-in period (coatings with lower surface roughness) showed lower friction values. Static COF in dry contact conditions was reduced from 0.271 to 0.173 (36%), kinetic COF in dry contact conditions was reduced from 0.247 to 0.157 (36%) and kinetic COF in seawater-lubricated contact conditions was reduced from 0.235 to 0.139 (41%).

The presence of seawater decreased the COF by 4.9% (for as-deposited coatings) and by 11% (for smoothed, runned-in coatings), which is beneficial. Seawater did not cause intensive corrosion, which would increase the friction, and only the lubricating effect of the seawater was present. Obtained values of the COF suggest that in some cases the boundary lubrication condition is obtained.

**Author Contributions:** Conceptualization, A.V.; methodology, A.V. and M.K.; validation, B.S. and A.B.; formal analysis, A.V.; investigation, M.K. and M.Z.; writing—original draft preparation, A.V.; writing—review and editing, R.N.; funding acquisition, J.P. and F.B. All authors have read and agreed to the published version of the manuscript.

**Funding:** This work has been performed as a part of activities within the projects 451-03-68/2022-14/200105 and TR 35021, supported by the Republic of Serbia, Ministry of Education, Science and Technological Development, and its financial help is gratefully acknowledged. Ružica Nikolić acknowledges the project “Innovative Solutions for Propulsion, Power and Safety Components of Transport Vehicles” ITMS 313011V334 of the Operational Program Integrated Infrastructure 2014–2020 and co-funded by the European Regional Development Fund. František Botko and Ján Piteľ acknowledge the project supported by the Slovak Research and Development Agency under the contract No. APVV-20-0514 and also the project VEGA 1/0080/20 granted by the Ministry of Education, Science, Research and Sport of the Slovak Republic. Collaboration through the CEEPUS networks CIII-BG-0703 and CIII-PL-0701 and bilateral Project 337-00-00111/2020-09/50 between Republic of Serbia and Republic of Slovenia is also acknowledged.

**Institutional Review Board Statement:** Not applicable.

**Informed Consent Statement:** Not applicable.

**Data Availability Statement:** Not applicable.

**Conflicts of Interest:** The authors declare no conflict of interest.

## References

1. Kandeve-Ivanova, M.; Vencl, A.; Karastoyanov, D. *Advanced Tribological Coatings for Heavy-Duty Applications: Case Studies*; Prof. Marin Drinov Publishing House of Bulgarian Academy of Sciences: Sofia, Bulgaria, 2016; pp. 9–37.
2. Brenner, A.; Riddell, G.E. Nickel Plating by Chemical Reduction. U.S. Patent 2532282, 5 December 1950.
3. Morcos, B.; Barnstead, M. Electroless nickel plating. *Prod. Finish.* **2011**, *75*, 44–48.
4. Colaruotolo, J.; Tramontana, D. Engineering applications of electroless nickel. In *Electroless Plating: Fundamentals and Applications*; Mallory, G.O., Hajdu, J.B., Eds.; Noyes Publications/William Andrew Publishing: Norwich, UK, 1990; pp. 207–227.
5. Gillespie, P. Electroless nickel coatings: Case study. In *Surface Engineering Casebook: Solutions to Corrosion and Wear-Related Failures*; Burnell-Gray, J.S., Datta, P.K., Eds.; Woodhead Publishing: Cambridge, UK, 1996; pp. 49–72.
6. Sahoo, P.; Das, S.K. Tribology of electroless nickel coatings—A review. *Mater. Des.* **2011**, *32*, 1760–1775. [[CrossRef](#)]
7. Uday Venkat Kiran, K.; Arora, A.; Ratna Sunil, B.; Dumpala, R. Sliding wear characteristics of as-deposited and heat-treated electroless Ni-P coatings against AISI E52100 steel ball. *Mater. Res. Express* **2019**, *6*, 036401. [[CrossRef](#)]
8. Mohamed, Y.S.; El-Gamal, H.; Zaghoul, M.M.Y. Micro-hardness behavior of fiber reinforced thermosetting composites embedded with cellulose nanocrystals. *Alex. Eng. J.* **2018**, *57*, 4113–4119. [[CrossRef](#)]
9. Zaghoul, M.M.Y.; Zaghoul, M.Y.M.; Zaghoul, M.M.Y. Experimental and modeling analysis of mechanical-electrical behaviors of polypropylene composites filled with graphite and MWCNT fillers. *Polym. Test.* **2017**, *63*, 467–474. [[CrossRef](#)]
10. Huang, H.-C.; Chung, S.-T.; Pan, S.-J.; Tsai, W.-T.; Lin, C.-S. Microstructure evolution and hardening mechanisms of Ni-P electrodeposits. *Surf. Coat. Technol.* **2010**, *205*, 2097–2103. [[CrossRef](#)]
11. Mucelin, K.J.; da Costa Gonçalves, P.; Hammes, G.; Binder, R.; Janssen, R.; Klein, A.N.; Biasoli de Mello, J.D. Tribological study of self-lubricating composites with hexagonal boron nitride and graphite as solid lubricants. In Proceedings of the 2nd International Brazilian Conference on Tribology—TriboBR 2014, Foz do Iguaçu, Brazil, 3–5 November 2014; pp. 3772–3781.
12. Khalaj, M.; Golkhatmi, S.Z.; Alem, S.A.A.; Baghchesaraee, K.; Azar, M.H.; Angizi, S. Recent progress in the study of thermal properties and tribological behaviors of hexagonal boron nitride-reinforced composites. *J. Compos. Sci.* **2020**, *4*, 116. [[CrossRef](#)]
13. Hussainova, I.; Kommel, L.; Kybarsepp, J.; Kimmari, E. Tribological properties of boron nitride based composites. In Proceedings of the World Tribology Congress III, Washington, DC, USA, 12–16 September 2005; Volume 1, pp. 53–54.
14. Huang, Z.; Zhao, W.; Zhao, W.; Ci, X.; Li, W. Tribological and anti-corrosion performance of epoxy resin composite coatings reinforced with differently sized cubic boron nitride (CBN) particles. *Friction* **2021**, *9*, 104–118. [[CrossRef](#)]
15. Kandeve, M.; Vencl, A.; Assenova, E.; Karastoyanov, D.; Grozdanova, T. Abrasive wear of chemical nickel coatings with boron nitride nano-particles. In Proceedings of the 11th International Conference in Manufacturing Engineering the “A” Coatings, Thessaloniki, Greece, 1–3 October 2014; pp. 319–325.
16. Parkinson, R. Properties and applications of electroless nickel. In *Nickel Development Institute Technical Series*; Nickel Development Institute: Toronto, ON, Canada, 1997; p. 10081.
17. Kennedy, F.E.; Gibson, U.J. Tribological surface treatments and coatings. In *Tribology Data Handbook: An Excellent Friction, Lubrication, and Wear Resource*; Richard Booser, E., Ed.; CRC Press: Boca Raton, USA, 1997; pp. 581–593.
18. Kandeve, M.; Svoboda, P.; Nikolov, N.; Todorov, T.; Sofronov, Y.; Pokusová, M.; Vencl, A. Effect of silicon carbide nanoparticles size on friction properties of electroless nickel coatings. *J. Environ. Prot. Ecol.* **2020**, *21*, 1314–1325.
19. Vencl, A.; Jakimovska, K.; Ivanova, B.; Ruzic, J.; Simeonov, S.; Kandeve, M. Static and kinetic friction of electroless Ni composite coatings. *J. Achiev. Mater. Manuf. Eng.* **2015**, *70*, 13–21.
20. Baibordi, A.; Amini, K.; Bina, M.H.; Dehghan, A. The effect of heat treatment temperature on the properties of the composite duplex electroless coating of Ni-P/Ni-B-BN containing boron nitride nanoparticles. *Kov. Mater.-Met. Mater.* **2014**, *52*, 263–268. [[CrossRef](#)]
21. Rac, A.; Vencl, A. *Metallic Materials of Plain Bearing Metallic Materials: Mechanical and Tribological Properties*; Faculty of Mechanical Engineering: Belgrade, Serbia, 2004; pp. 1–16. (In Serbian)
22. Davis, J.R. (Ed.) *Surface Engineering for Corrosion and Wear Resistance*; ASM International: Metals Park, OH, USA, 2001; pp. 43–86.
23. Ivković, B.; Djurdjanović, M.; Stamenković, D. The influence of the contact surface roughness on the static friction coefficient. *Tribol. Ind.* **2000**, *22*, 41–44.
24. Niu, Q.L.; Zheng, X.H.; Ming, W.W.; Chen, M. Friction and wear performance of titanium alloys against tungsten carbide under dry sliding and water lubrication. *Tribol. Trans.* **2013**, *56*, 101–108. [[CrossRef](#)]
25. Ri, J.H.; Ripeanu, R.G. Evaluation of the wear and corrosion resistance of coated parallel gate valve. *Tribol. Mater.* **2022**, *1*, 11–20. [[CrossRef](#)]
26. Miura, K.; Takata, K.; Fujiwara, K.; Shimosako, Y. Characteristics of static friction in sea water on universal joint member materials. *J. Soc. Mater. Sci. Jpn.* **2005**, *54*, 519–523. (In Japanese) [[CrossRef](#)]
27. Zakowski, K.; Narozny, M.; Szocinski, M.; Darowicki, K. Influence of water salinity on corrosion risk—The case of the southern Baltic Sea coast. *Environ. Monit. Assess.* **2014**, *186*, 4871–4879. [[CrossRef](#)] [[PubMed](#)]
28. Vencl, A.; Šljivić, V.; Pokusová, M.; Kandeve, M.; Sun, H.; Zadorozhnaya, E.; Bobić, I. Production, microstructure and tribological properties of Zn-Al/Ti metal-metal composites reinforced with alumina nanoparticles. *Int. J. Met.* **2021**, *15*, 1402–1411. [[CrossRef](#)]
29. Wang, C.; Ye, Y.; Guan, X.; Hu, J.; Wang, Y.; Li, J. An analysis of tribological performance on Cr/GLC film coupling with Si<sub>3</sub>N<sub>4</sub>, SiC, WC, Al<sub>2</sub>O<sub>3</sub> and ZrO<sub>2</sub> in seawater. *Tribol. Int.* **2016**, *96*, 77–86. [[CrossRef](#)]
30. Ye, Y.; Wang, C.; Wang, Y.; Liu, W.; Liu, Z.; Li, X. The influence of different metallic counterparts on the tribological performance of nc-CrC/GLC in seawater. *Surf. Coat. Technol.* **2017**, *325*, 689–696. [[CrossRef](#)]